aerospace

MDPI

Review

Ice Accretion on Rotary-Wing Unmanned Aerial Vehicles—A Review Study

Manaf Muhammed * and Muhammad Shakeel Virk

Arctic Technology & Icing Research Group, UiT—The Arctic University of Norway, 8514 Narvik, Norway
* Correspondence: manaf.muhammed@uit.no

Abstract: Ice accretion on rotary-wing unmanned aerial vehicles (RWUAVs) needs to be studied separately from the fixed-wing UAVs because of the additional flow complexities induced by the propeller rotation. The aerodynamics of rotatory wings are extremely challenging compared to the fixed-wing configuration. Atmospheric icing can be considered a hazard that can plague the operation of UAVs, especially in the Arctic region, as it can impose severe aerodynamic penalties on the performance of propellers. Rotary-wing structures are more prone to ice accretion and ice shedding because of the centrifugal force due to rotational motion, whereby the shedding of the ice can lead to mass imbalance and vibration. The nature of ice accretion on rotatory wings and associated performance degradation need to be understood in detail to aid in the optimum design of rotary-wing UAVs, as well as to develop adequate ice mitigation techniques. Limited research studies are available about icing on rotary wings, and no mature ice mitigation technique exists. Currently, there is an increasing interest in research on these topics. This paper provides a comprehensive review of studies related to icing on RWUAVs, and potential knowledge gaps are also identified.

Keywords: atmospheric icing; rotary-wing UAV; propellers; aerodynamic penalties; IPS

Citation: Muhammed, M.; Virk, M.S. Ice Accretion on Rotary-Wing Unmanned Aerial Vehicles—A Review Study. *Aerospace* **2023**, *10*, 261. https://doi.org/10.3390/aerospace10030261

Academic Editors: Ning Zhao and Hirotaka Sakaue

Received: 10 January 2023
Revised: 27 February 2023
Accepted: 3 March 2023
Published: 8 March 2023

1. Introduction

Unmanned aerial vehicles (UAVs) have grown in popularity since 1990, with extremely rapid development and research in the field. UAVs were initially introduced for military applications such as intelligence, targeting and battle damage assessment, surveillance, and reconnaissance. Later, drones revealed their potential civil applications, such as for search and rescue missions, exploration, security and surveying of oil pipelines, agricultural applications, and power and nuclear plant inspection [1]. Recently, the commercial applications of UAVs have been exposed, such as package delivery, air metros, air taxis, etc. [2]. It is estimated that by 2030, UAVs will have delivered 1.4 billion express packages and that urban air mobility vehicles will have operated 50 million trips [3]. In 2022, Villeneuve [4] presented the concept and a design for the use of drones to spray anti-icing fluids on aircraft. UAVs are classified based on their mode of propulsion as fixed-wing, flapping-wing, and rotary-wing UAVs. The major advantage of rotary-wing UAVs (RWUAVs) over fixed-wing UAVs is their vertical take-off and landing (VTOL) capability, which reduces the need for a runway. Due to their small size, simple structure, excellent agility, fast maneuvering, and VTOL capabilities, quadcopter UAVs have become increasingly appeal in recent years. They are ideal for flight operations requiring balanced controls. Due to their simplicity and low cost, research and development on quadrotors has recently increased [5]. Their hovering capability, ability to carry heavy payloads (compared to a fixed-wing UAVs of similar gross weight), and stability in strong winds make RWUAVs suitable for commercial applications. However, high power requirements and complex electrical and mechanical systems are significant challenges for rotary-wing UAVs compared to fixed-wing UAVs [6].

Fixed-wing UAVs generate lift with the help of a fixed aerodynamic wing, whereas RWUAVs generate lift force against gravity by rotating wings or rotors. The major components of an RWUAV are the frame structure, propellers, flight control card, brushless

DC motors, electronic speed controller (ESC), battery, and flight controller. The operating parameters of UAVs such as speed, altitude, etc., are remotely controlled by an operator. The transmitted instructions are received by an onboard flight controller, which translates them into control signals. These control signals enhance or decrease lift/thrust by altering the amount of current delivered by the ESC to the BLDC motors. Each propeller is connected to a motor, and each motor is connected to its ESC. Changes in the direction and speed of these rotors helps in maneuvering the vehicle [5]. The aerodynamics of rotatory wings are extremely challenging compared to the fixed-wing configuration. The rotatory motion of the wings/blades/propellers makes the problem nonlinear, thereby increasing the numerical complexity. Experiments are also challenging and expensive to conduct. As a result, most research focuses on studies on single-propeller-blade configurations. However, changing propeller blade profiles along their length, twisting, and tapering further complicate the problem.

The use of unmanned aircraft systems (UAS) has grown steadily in the United States and worldwide in recent years. There are currently 1.65 million recreational and commercial drones (250 g < UAV < 25 kg) in the active UAS fleet, which is expected to increase to as much as 2.31 million by 2024. The number of large active UAVs (>250 kg) was 284 in 2020 and is expected to increase to 339, with a total number of 12,500 flights by 2025. In 2021, the Federal Aviation Administration (FAA) awarded USD 19.1 million to various universities in the United States for UAV research in the form of in 57 research grants [7]. The use of commercial drones in Germany is expected to increase by 525% between 2019 and 2030, with 721,000 private UAVs already been in operation. As the volume of UAV traffic increases, understanding the possible hazards of UAV operation is required to ensure safe flights. Comparing to manned aircrafts, UAVs are more likely to experience loss of control during flight, accidents and incidents during take-off and landing, as well as equipment related problems [8]. Electromechanical failures are the major cause of UAV accidents [9]. According to the Australian Transport Safety Bureau (ATSB), rotary-wing aircraft have a higher accident rate than fixed-wing aircraft. They also consider maneuvering and cruising as the most common phases of flight for rotary-wing aircraft accidents [10].

Ice accretion on the propeller/rotors can be considered a major threat for the operation of RWUAVs in ice-prone regions, leading to a loss of control and catastrophic failures. A proportion of 25% of US military UAV operations in North America encountered icing hazards that hampered their mission success [11]. According to a weather analysis performed by Lundby et al. [12] in two major Danish cities on 2019, the operational time of the DJI Phantom IV RWUAV is limited to only 54% of the year due to adverse weather. The operational time of its fixed-wing counterparts and other large aircraft is much longer. In 2021, Sørensen [13] reported that from September through May, icing conditions are present from 35% to more than 80% of the time in northern Europe. Potential icing conditions exist in Norway throughout the year, with the frequency of such conditions ranging from 30 to 95% depending on the season. As per the norms, the operational altitude of small multirotor UAVs is limited to 120 m, while large UAVs can fly at altitudes of up to 3000 m [14]. Low cumuliform clouds, ice fog, and freezing drizzle are present at these altitudes and can lead to severe ice accretion.

Ice can accumulate on any exposed surface of a UAV, including the wings, propellers, arm, and even payloads such as cameras. Tramposch [15] studied droplet impingement on an octocopter in 2021 and discovered that the leading edge of the propeller blade has the highest droplet impingement rate, followed by the pressure side and the suction side of the propeller blade. As a result, the leading edge of the propeller blade is most vulnerable to ice accretion. Because of the combined effect of shear and centrifugal forces, the nature of ice accreted on propeller blades is more ragged than that on their fixed-wing counterparts. Thus, the ice can significantly impact the aerodynamic performance of an RWUAV compared to a fixed-wing UAV. Furthermore, due to the centrifugal loads, ice accumulated on propellers has an increased tendency to shed. Ice increases weight and drag, creates excess vibration, and introduces mass and aerodynamic unbalance when the

ice sheds off [16]. Icing studies on rotary-wing structures are still challenging; the major challenges were discussed by Cao in [17].

Ice accretion can be studied mainly using flight tests, experiments (lab and field), and numerical simulation. Flight tests are risky and costly, as they can destroy the vehicle. Furthermore, the short-range operation of UAVs forces the researcher to wait for suitable weather conditions for the experiments rather than seeking them out. Icing conditions created in icing tunnels for experiments require calibration and are still unable to accurately recreate natural icing conditions. The major challenges in numerical simulations are:

1. Compared to a fixed-wing configuration, the flapping, leading, and lagging (lead–lag) of rotating wings cause the behavior of water on the blade surface to be unpredictable;
2. The complexity of flow around the blade: (a) The velocity of the flow varies from root to tip of the rotary wing [18]; (b) the impact of complex physics of rotary flow such as the wakes, blade–vortex interaction, and complex turbulence on the ice accretion behavior;
3. The surface roughness due to ice accumulation varies significantly across the blade's surface, which can affect the heat transfer and, eventually, the shape of accreted ice;
4. The centrifugal force and the ice-shedding effects near the blade tip are also difficult to model numerically [18].

A 1981 FAA helicopter icing review [19] concluded that rotorcraft icing and ice protection systems present a unique set of aerodynamic and thermodynamic problems that cannot simply be adapted to existing ice protection system (IPS) designs developed for fixed-wing aircraft. Ice accretion on UAV rotors and propellers needs to be studied separately from helicopters and wind turbines. The low operating Reynolds number and the sensitivity of UAV blade profiles to mild changes in the flow behavior caused by ice roughness make UAV propeller icing unique. Furthermore, the blades are often subjected to sudden changes in the flow and rotational conditions. RWUAVs can be more vulnerable to icing and severe icing hazards than fixed-wing UAVs of similar gross weight due to following reasons.

1. They typically lack the altitude required to escape hazardous icing weather [20];
2. RWUAV operations require long hovering periods in a single location [20];
3. The rotational motion of the rotors results in the formation of more rough and ragged ice structures at the leading edge of propellers, resulting in a considerable increase in profile drag and a reduction in the lift-to-drag ratio, thereby increasing the torque and power requirements;
4. The high rotational speed of the rotor generates large values of centrifugal forces, especially near the tips, resulting in ice shedding. The uneven ice distribution caused by shedding leads to rotor imbalance and severe vibrations;
5. The periodic changing of the blade profile, sectional angle of attack, and uneven distribution of relative velocities along a rotor blade causes a dramatic variation in ice accretion mass [18] and complicates rotor icing by changing the spanwise surface temperature variations;
6. The higher collection efficiency of thin rotor airfoils coupled with high tip speeds makes them accrete ice faster than thicker airfoils of fixed-wing UAVs [21];
7. Limitations on battery capacity and weight constraints, along with the propeller's rotary motion, demand unique ice mitigation systems for RWUAVs;
8. The lightweight and thin structure of RWUAVs makes them physically more vulnerable to ice.

Thus, ice accretion studies on rotary wings are extremely challenging compared to studies on fixed-wing configurations.

The nature of the ice formed when supercooled water droplets impinge on a surface depends on how rapidly the latent heat of fusion can be released into the ambient air [22]. Glaze ice is formed at temperatures close to the freezing point (and for high values of liquid water content), when the heat transfer is insufficient to remove all the latent heat of fusion released during the solidification process of the droplets impinging on the surface.

Thus, only a portion of the impinged droplets freezes into ice, and the remaining droplets can run back to the surface. This type of ice is characterized by high density (900 kg/m^3), very high adhesion to the surface, and clear and smooth appearance. Rime ice is formed at very low temperatures (and for low *LWC* values), when the heat transfer is sufficient to remove all the latent heat of fusion for the droplets impinging on the surface, and it freezes instantly. It is characterized by low density (200–700 kg/m^3) and a white, opaque, and rough appearance. Mixed ice is formed in the temperature range between glaze and rime-ice conditions, and it exhibits the characteristics of both rime and glaze ice. Surface water transport is primarily driven by aerodynamic shear on fixed-wing UAVs, whereas it is driven by both aerodynamic shear and centrifugal forces on rotating propellers. Because the droplets freeze on impact, the effect of centrifugal force is minimal for rime ice, and the ice formed under these conditions closely follows the propeller surface. For glaze ice, the unfrozen water droplets are carried mainly along the chord in the case of fixed-wing UAVs. For rotating propellers, along with chordwise transport, the action of centrifugal force results in water transportation along the span. The water is transported along the leading edge from the root to the tip of the blade, linearly increasing ice thickness in that direction. The higher velocity at the blade tip accelerates the ice accretion process near the blade tip. Furthermore, higher *LWC* values lead to the formation of "feathers" growing outside the blade tip [23]. When the ice mass is increased at the blade tip, the centrifugal force is increased, and once it overcomes the ice adhesion force, the ice starts shedding.

The performance of a propeller is mainly characterized by its thrust coefficient (C_T), power coefficient (C_p), and propeller efficiency (η). These parameters are plotted as a function of the advance ratio (J), which is the ratio of freestream velocity of airflow (U) to the propeller tip speed (See Equation (1)).

$$C_T = \frac{T}{\rho n^2 D^4}\ ,\ C_p = \frac{P}{\rho n^3 D^5},\ J = \frac{U}{nD},\ \eta = J\frac{C_T}{C_p} \tag{1}$$

where ρ is the density of the fluid, n is the rotational speed of the propeller, and D is the diameter of the propeller. The power (P) can be calculated according to the mechanical power $(P = 2\pi nQ)$ or electrical power $(P = UI)$, where Q is the torque, and I is the current. The centrifugal force of the rotating wing can act as a natural deicing method, as it helps in ice shedding, but the unsymmetric shedding of ice can lead to mass imbalance in propellers and can result in failures [24]. Thus, the icing of rotary-wing UAVs needs to be studied separately from that of fixed-wing UAVs. The nature of ice accretion on rotatory wings and associated performance degradation needs to be understood in detail to aid in the optimum design of rotary-wing UAVs, as well as to develop adequate ice mitigation techniques. Only limited number of research studies are available about icing on rotary-wing UAVs, and no mature ice mitigation technique exists. Now a days there is an increasing interest in research related to these topics, and a review of existing knowledge and identification of knowledge gaps will be beneficial for future researchers. The existing wisdom about ice accretion on fixed-wing UAVs was reviewed by Muhammed and Virk [25] in 2022. This paper provides a comprehensive review of studies related to icing on RWUAVs, and potential gaps are identified.

2. Ice Accretion on Rotary-Wing UAVs

2.1. Ice Accretion on RWUAVs during Flight Tests

In 2017, Meteomatics engineers [26] studied ice accretion on a RWUAV (Meteodrone) under different icing conditions. Flight tests were conducted outdoors during winter and on an indoor ski slope under two different icing conditions: one at an altitude of 565 m with atmospheric temperature of $(T_\infty) = -2$ °C and relative humidity of 100% and another at an altitude of 534 m with $T_\infty = -2.5$ °C and relative humidity of 95%. Propeller icing was observed during both the flight tests, with a considerable increase in power input. In 2017, Avery [27] also observed ice accretion on the trailing edge of the propeller blades of a 3DR solo multirotor UAV during a routine flight. In 2021, Siddique [28] performed in-flight

testing of a Sonicmodell Skyhunter UAV under adverse weather conditions. The tests were conducted at the Iowa State University's Bio Century Research Farm (BCRF) under calm, windy, and icing flight conditions. The T_∞ value observed during the icing condition test was -1.5 °C, and it led to the formation of glaze ice on the wing leading edge and propellers. Water runback rivulets were visible on the top surface of the wing downstream of the leading edge. The propellers were heavily iced, forming horns and ridges on the pressure and suction sides. A dramatic increase in power of 240% was observed during ice accretion compared to the calm weather condition and even led to increased battery consumption. Dhulipalla [29] performed flight testing of a Quadcopter UAV under windy and icing conditions at $T_\infty = -3$ °C. Glaze-ice formations were observed on the propellers, and 0.486 g of ice was accreted with 80 s of icing, resulting in a power increase of 98%.

The observations made during these flight tests indicate that ice accretion on RWUAVs can result in a significant increase in power requirements, potentially jeopardizing mission success. Therefore, it is necessary to thoroughly investigate ice accumulation on RWUAVs to understand its underlying physics and to create ice mitigation methods that are compatible with RWUAVs. The limitations of using flight tests for such purposes are discussed in [25]. Lab experiments in icing tunnels and numerical icing simulations can be considered more suitable for such purposes. Below, we present a summary of the current understanding of the characteristics of ice accreted on RWUAVs under various meteorological situations as determined by experimental icing experiments.

2.2. General Characteristics of RWUAV Ice Accretion Based on Icing Tunnel Experiments

For fixed-wing UAVs, the nature of the formed ice depends primarily on free-stream velocity (V_∞), atmospheric temperature (T_∞), liquid water content (*LWC*), the droplet median volume diameter (MVD), angle of attack (α), Reynolds number (*Re*), the material, and the geometry of the structure (airfoil, surface roughness, chord, and mean effective camber) [25]. However, for rotating propellers, additional factors such as the propeller rotating speed (rpm), advance ratio, tilt angle, and angle of side slip can also affect the ice accretion behavior. During icing tunnel tests on fixed wings, the final ice shape can be obtained by either tracing on paper or by using 3D/4D scanning techniques [30,31]. Due to the propeller rotation and ice shedding in rotating propellers, accurately obtaining the ice shapes is more challenging and requires sophisticated methodologies. In the majority of previous works, only photographs of accumulated ice obtained after trials have been included [26,32]. Some of photographs were taken after ice-shedding events; therefore, they cannot be trusted as credible information about the traits of ice that was formed. Most studies on propeller icing concentrate on measuring the variation in aerodynamic coefficients rather than the ice morphologies, owing to the limitations of transient imaging. The experimental studies done by Liu [16] at the Iowa State University Icing Research Tunnel (ISU-IRT) in 2017 captured transient ice profiles using a 'phase-locked' high-speed imaging technique. These studies were performed on a 1:14 scaled three-blade rotating UAV propeller. In 2018, Ning [33] performed studies similar to those of Liu [16] by conducting experiments under a broader range of environmental conditions.

Followed by observation of ice during flight tests, in 2017, Meteomatics engineers [26] performed experimental studies at the Vienna Climatic Wind Tunnel (VCWT). These tests were conducted under six different weather conditions considering EASA CS25/CS29 Appendix C guidelines [34], and pictures of the final ice shapes were published. Based on the observations made during these experimental studies, it can be inferred that the nature of the formed ice primarily depends on T_∞ and *LWC* values rather than other parameters. In 2019, Benmeddour [32] reported that changes in *LWC* have a more pronounced effect on icing characteristics than changes in MVD. When $T_\infty \leq -15$ °C, the formed ice always exhibits rime-ice characteristics, even with high values of *LWC* up to 2 g/m^3. The ice formed under rime-ice conditions closely follows the airfoil section of the propeller without disturbing the streamline behavior. Furthermore, due to the immediate freezing of water droplets upon impingement, no water transport along the leading edge or run-

back downstream of the leading edge occurs, which indicates that rime-ice formation is influenced neither by the centrifugal force due to rotation nor by the aerodynamic shear forces; it depends primarily on the water collection efficiency of the leading edge. Further impingement of water droplets results in the thickening of the ice layer along the leading edge, with the growth of ice feathers. The ice feathers formed along the leading edge induce flow separation downstream of the ice layer and prevent water droplet impingement. Thus, no further increase in ice extent is observed, and only the ice layer that reaches out into the outer flow continues to grow [16]. Ning [33] observed that an increase in the value of *LWC* from 0.5 to 2 g/m^3 at $T_\infty = -15$ °C resulted in an increased ice accretion growth along the leading edge of the propeller; however, the characteristics of the ice remained consistent with rime, as shown in Figure 1. It can also be observed that the thickness of the ice increases in a linear fashion from the root to tip of the blade [35]. This may be due to the increase in droplet impingement with increased effective velocity from root to tip. Han [36] conducted experimental research on a 9443 two-blade propeller in 2021 in order to comprehend the ice accretion process in a typical rime- and glaze-ice environment. Rime ice covered a smaller portion of the propeller leading edge than glaze ice, and the formed ice was smooth and aerodynamic. Ice-shedding events are less common under rime-ice conditions, resulting in a significant increase in leading-edge ice formation. For both cases, the growth of leading-edge ice thickness has a linear relationship with time, and the linearity is especially apparent under rime-ice conditions due to the instantaneous freezing of water.

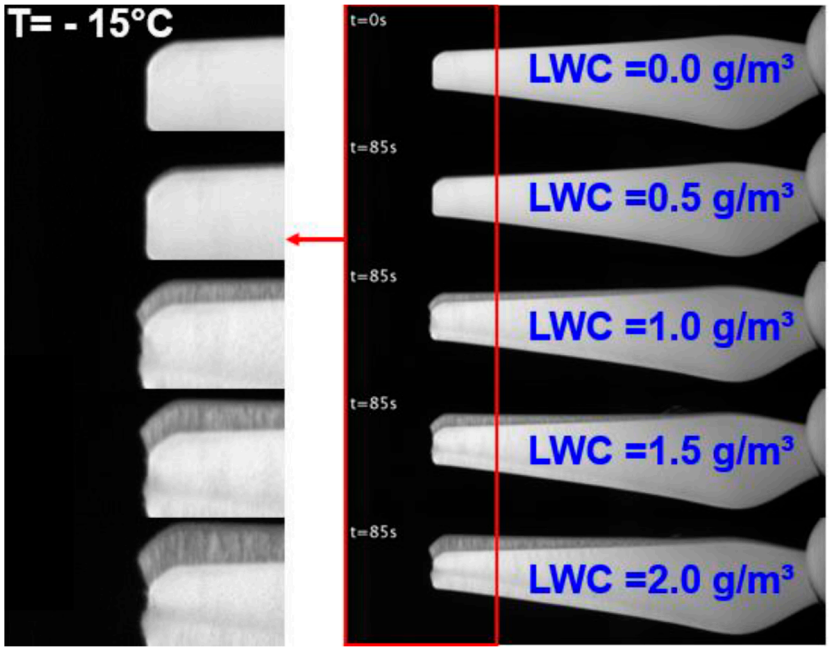

Figure 1. Ice accretion at $T_\infty = -15$ °C for different *LWC* values [33].

When the ambient temperature is very close to the freezing point at $T_\infty = -2$ °C, the heat transfer process is insufficient to remove all the latent heat of fusion in the impinged droplets. Therefore, only a part of the droplet freezes upon impingement, and the remaining water is transported along the blade surface by the action of aerodynamic shear and centrifugal forces. The water droplets are transported downstream by the action of shear forces. Due to the action of centrifugal force, the water droplet's behavior becomes three-dimensional, and it is transported both chordwise and spanwise. The water transported radially from root to tip results in the formation of 'pin-shaped' ice structures near the blade tip. With further water impingement or increased *LWC*, the 'pin-shaped' ice structures become more prominent. An *LWC* value of even 0.6 g/m^3 results in the formation of complex "lobster-tail-like" ice structures near the blade tip [26], as shown in Figure 2.

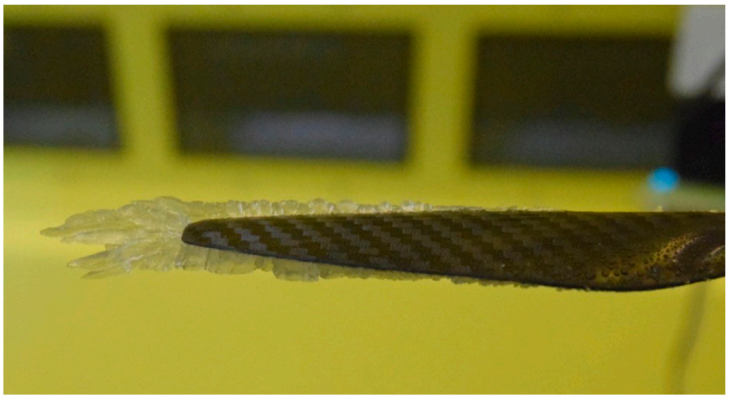

Figure 2. Ice accretion at $T_\infty = -2$ °C for $LWC = 0.6$ g/m^3 [26].

In the atmospheric temperature range of −4 °C to − 10 °C, the nature of the formed ice is heavily influenced by the *LWC* values. The effectiveness of the heat transfer process in eliminating the latent fusion generated during the solidification of impinged droplets is influenced by the interaction between atmospheric temperature and *LWC* values. The extent to which the latent heat of fusion is removed determines the type of ice accreted. In 2018, Ning [33] experimentally studied the effect of *LWC* on the nature of propeller ice accretion at $T_\infty = -4$ °C by increasing the *LWC* from 0.5 to 2 g/m^3. At an *LWC* of 0.5 g/m^3, a thin layer of rime ice was formed along the leading edge of the propeller, and the geometry of the ice closely followed the propeller geometry. As the value of *LWC* was increased to 1 g/m^3, the nature of the ice changed to mixed, and the color of the ice became transparent. However, a small portion of the impinged droplets that did not freeze on impact was carried by the action of centrifugal force, as well as wind shear, and tiny ice growth outside the blade tip was observed. There were no rivulets, and the ice shape followed the propeller geometry. When the value of *LWC* was increased to 1.5 g/m^3, more water was carried to the tip by the forces and formed ice. With a further increase in *LWC* to 2 g/m^3, typical glaze-ice characteristics were observed, with the presence of rivulets and complex "pin-shape" structures bent towards the trailing edge at the blade tip, as shown in Figure 3. At −8 °C, the ice structure followed the propeller geometry and was similar to that at −4 °C, except for the fact that ice growth at the tip was only observed for $LWC \geq 1.5$ g/m^3. "Pin-shaped" glaze ice was observed at the blade tip for $LWC = 2$ g/m^3, but its size was smaller than that at −4 °C. In 2017, Liu [16] observed that at $T_\infty = -5$ °C and $LWC = 1$ g/m^3, water transport was affected by both shear and centrifugal force. Water transport due to shear force results in water runback, thereby increasing the icing extent along the propeller surface, whereas transport due to centrifugal force results in "needle-shaped" ice structures at the blade tip. However, ice accretion was mainly observed along the leading edge of the propeller blade and conformed with the propeller geometry. Therefore, the nature of accreted ice can be considered as mixed ice under these conditions. Such mixed ice characteristics were also observed in combinations of $T_\infty = -5$ °C, $LWC = 0.5 \frac{g}{m^3}$ and $T_\infty = -10$ °C, $LWC = 1.4 \frac{g}{m^3}$. An increase in *LWC* to 2 $\frac{g}{m^3}$ at $T_\infty = -5$ °C results in glaze ice with more jagged ice features and increased roughness because of the significant increase in the water content. More complex ice features are formed such that the "needle-shaped" ice transforms into a "lobster-tail-like" ice structure (see Figure 4). In 2021, Han [36] also observed the formation of pin-shaped ice structures on the propeller blade tip under glaze-ice conditions. Due to the comparatively moderate centrifugal force at the wing root, ice shedding near the propeller root was delayed, resulting in the creation of an "ice cone".

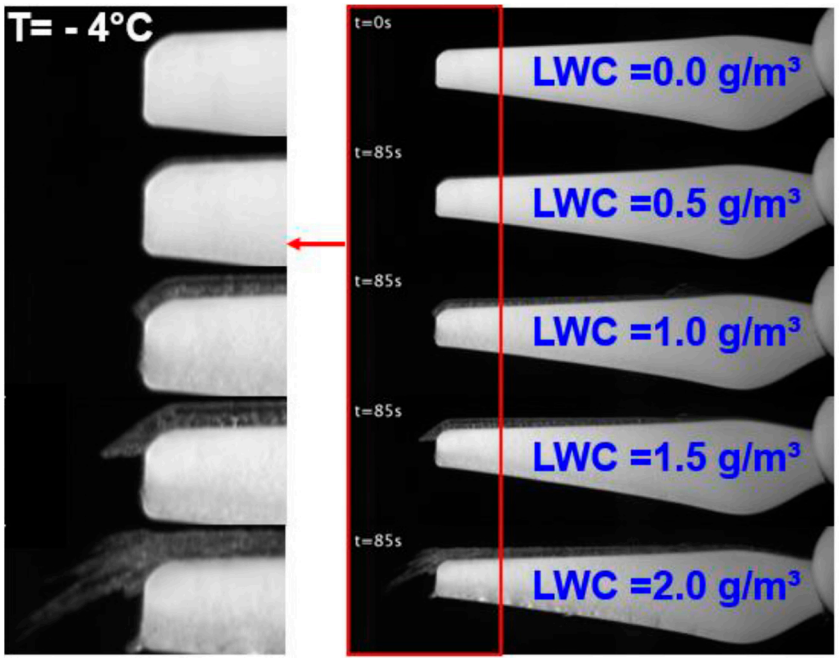

Figure 3. Ice accretion at $T_\infty = -4$ °C for different *LWC* values [33].

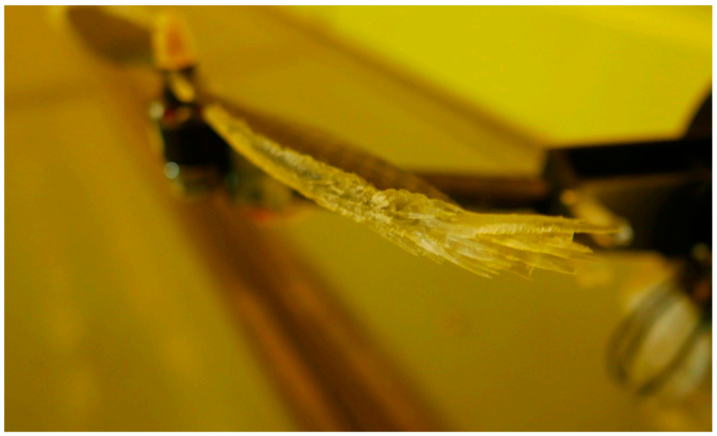

Figure 4. "Lobster-tail-like" ice structures formed at $T_\infty = -4$ °C for high *LWC* values [26].

Discussion: Transportation of water droplets on the surface of a rotating propeller is influenced by the action of both shear force and centrifugal force. The variation of effective velocity from root to tip of the blade influences the droplets' collision efficiency. The complex interplay between T_∞ and *LWC* determines the amount of unfrozen droplets. V_∞ and RPM can affect the aerodynamic heating of the propeller surface, which can also influence the freezing of impinged droplets. However, the effect of aerodynamic heating on RWUAV ice accretion has not been studied in detail and represents a research gap. The influence of MVD on ice shape is considered negligible when the droplet size is limited to FAR 25 regulations (up to 40 µm). The influence of other meteorological conditions such as *Re*, RPM, V_∞, α, advance ratio, and the material and geometry of the structure (airfoil, surface roughness, chord, and mean effective camber) on the nature of RWUAV ice accretion is also not yet fully understood due to transient imaging limitations. Complex ice structures that impede the aerodynamic flow over the surface are formed with high T_∞ values (near the freezing point) and high *LWC* combinations. Aerodynamic penalties of RWUAV icing under various meteorological conditions are reviewed in the following section.

3. Effect of Icing on the Aerodynamic Performance of a Propeller

In 2018, experimental investigations were performed by Yan et al. [37] to study the performance of a multirotor coaxial UAV under glaze icing conditions. For a propeller rotating at constant RPM in an icing cloud, the thrust was observed to degrade with time due to ice accretion. The loss of thrust demands an increase in rotor speed to compensate for the altitude loss, thereby increasing the torque and power requirements. The thrust decreases by 27.58% for the first 60 s of ice accretion, and the power consumption increases drastically by 184%. The reason for such a difference in thrust loss and power increase is that ice shape mainly reduces the aerodynamic lift-to-drag ratio. The drag force increases due to the increase in surface roughness or flow separation induced by the complex ice structures. Along with drag, the mass of the accreted ice also contributes to the increased power requirements. Therefore, a slight decrement in thrust due to icing can significantly impair the power performance and flight endurance. The effect of various environmental conditions on ice accretion of propellers is reviewed below.

3.1. Effect of Atmospheric Temperature

As discussed in Section 2, atmospheric temperature can be regarded as one of the most influential factors in determining the nature of ice accreted on a UAV propeller. Depending on the type of accreted ice, the surface roughness and flow characteristics vary significantly, affecting the propeller's aerodynamic performance. The aerodynamic forces acting on the propeller under icing conditions show significant fluctuations with time and are highly unsteady [16]. Under rime-ice circumstances ($T_\infty = -15\ ^\circ\mathrm{C}$), an initial rise in thrust force is typically noted upon ice accumulation. This is because ice accretion on the leading edge of the propeller causes an effective extension in chord length (lifting surface) due to the streamlined thickening of ice in the leading edge. Liu [16] in 2017 observed an increase in thrust coefficient by 15% upon icing for an initial 90 s. Keeping the *LWC* and MVD constant, similar observations were made during mixed ice temperatures ($T_\infty = -5\ ^\circ\mathrm{C}$), with a 13% increase in mean thrust. Drag increases due to the increase in roughness and mass, as well as flow separation effects. Because of the increase in aerodynamic drag and total rotating mass, the input power (C_p) increases upon ice accretion for both rime (20%) and mixed (30%) ice. In 2018, Ning [33] observed that the lift decreases more rapidly with an increase in temperature at a low *LWC* value of 0.5 $\frac{\mathrm{g}}{\mathrm{m}^3}$ (rime-ice characteristics were observed at this *LWC* for all considered T_∞ values). However, the trend is opposite at higher *LWC* values, although more complex ice structures were observed at warmer temperatures. One of the reasons for this disparity may be the fact that extended ice structures under glaze-ice conditions on the tip of the propeller increased the aerodynamic surface area and modified the tip vortex formation favorably (ogee tip) [38]. Increases in the ice mass of the rime ice may be another reason, although mass was not measured in these studies. The initial thrust increase was also not reported in the studies, although the experimental conditions were similar to those reported by Liu [16]. The maximum lift degradation was $-15\ ^\circ\mathrm{C}$ (19%) compared with the no-ice condition. The power requirements were observed to increase as the temperature increased, possibly due to the corresponding increase in drag due to rough ice structures formed at mixed ice temperatures. Power consumption increases linearly with time under rime ice and mixed ice conditions but quadratically under glaze-ice conditions. Ice accretion doubles the power requirements at $T_\infty = -15\ ^\circ\mathrm{C}$, whereas it increased by 5 times for the glaze-ice condition at $T_\infty = -4\ ^\circ\mathrm{C}$. Thus, the power requirement is determined not only by the thrust loss but also by the increase in drag caused by surface roughness.

In 2020, Benmeddour [32] performed experimental icing studies on a two-blade propeller with three different diameters and observed that rime ice temperature ($-12\ ^\circ\mathrm{C}$) and mixed ice temperature ($-5\ ^\circ\mathrm{C}$) resulted in an increased thrust reduction rate compared to the glaze icing condition at $-2\ ^\circ\mathrm{C}$. At $-2\ ^\circ\mathrm{C}$, significantly less ice was accreted on the smaller blade ($10''$ diameter), and no ice formation was observed on the medium-sized ($12''$ diameter) and larger blade ($14''$ diameter). This may be due to the increased aerodynamic

heating due to higher propeller rotating speeds (8000 rpm) and V_∞ used in these studies. Thus, at a temperature of -2 °C, the thrust appeared to remain constant for 10 times longer duration than the same at -12 °C before it started declining. At -12 °C and -5 °C, the thrust declined to 50% in less than 50 s, whereas the thrust was retained for a much longer duration at -2 °C. The power requirements were almost doubled when the free stream temperature changed from -2 °C to -12 °C. In 2021, Han [36] observed that thrust was diminished due to icing under glaze-ice conditions until ice shedding took place. When ice shedding took place, the thrust briefly rose, then fell until it reached its previous position again. Rotation speed fluctuation is also rather large under glaze-ice conditions because ice shedding occurs frequently. The safety of flights may be at risk from this type of influence on the control system. The initial thrust did not vary considerably in the rime-ice scenario. Following the first ice shedding, it began to recede. This may be due to the fact that the ice accumulated after shedding is no longer aerodynamic.

In 2021, Muller [39] performed numerical ice accretion studies on a Meijzlik 21 × 10 EL UAV propeller using the FENSAP-ICE software package. Simulations were performed under three different meteorological conditions at $T_\infty = -2$ °C, -5 °C, and -15 °C, with the propellers rotating at 5000 rpm and $V_\infty = 25$ m/s. Supporting the observations of Benmeddour [32], ice accretion was observed only on the central part of the propeller at $T_\infty = -2$ °C, and no ice was observed near the tip, which can be attributed to the high stagnation temperature near the tip due to increased velocity. Similarly, ice was not observed near the tip at $T_\infty = -5$ °C, but ice accreted on the remaining area of the propeller. Full-length rime-ice formation was observed at $T_\infty = -15$ °C. To analyze the performance of the propeller, the final ice shapes obtained from the FENSAP-ICE simulations were simulated in ANSYS Fluent. The lowest performance degradation was observed for glaze ice at $T_\infty = -2$ °C, with a thrust reduction of 4.1% and a power increase of 9.1%. The mixed ice condition at $T_\infty = -5$ °C predicted the highest performance penalties, with a thrust reduction of 47 % and a power increase of 44 %. At $T_\infty = -15$ °C, the thrust reduction was 9.5 %, with a power increase of 29.5 %. In 2022, Muller [40] reported that the efficiency of the propeller was lower in the intermediate temperature range of -5 °C to -15 °C than at -2 °C or -20 °C. The fastest performance loss rate was observed at -10 °C. In contrast, in 2022, Karpen [35] reported a faster thrust reduction rate for glaze ice $(0\ ^\circ\mathrm{C})$ than rime ice $(-10\ ^\circ\mathrm{C})$. The rate of thrust reduction was observed to be 1N per 100 s for glaze ice and 1N per 250 s for rime ice. The reason for such a contradiction may be the low V_∞ value (2.2 m/s) used in his studies, which can considerably reduce the aerodynamic heating. In 2022, Hylmar [41] observed that the mass of the ice accumulated in 35 s of icing at -10 °C and -15 °C was 56% and 113% more, respectively, than at -5 °C. Such high levels of mass at a lower temperature may explain the increased power requirements under rime-ice conditions despite the complexity of ice structures at warmer temperatures. At $-5, -10,$ and -15 °C, the corresponding decreses in thrust were 29.4, 88.4, and 91.4%, with increases in power of 51.6, 457.4, and 505.3%, respectively. In the case of ice accretion studies on supercooled large droplets (SLDs), faster performance degradation was observed under glaze-ice than rime-ice conditions [42].

3.2. Effect of LWC

The change in *LWC* values has a profound impact on the nature of accreted ice and propeller performance. In 2017, Liu [16] observed a significant decrease in the thrust force (70%) for glaze ice with increased *LWC* due to the formation of more complex ice structures, as mentioned above. Correspondingly, the power coefficient also increased exponentially to 250% within 90 s of the icing event. This may be due to the tremendous increase in aerodynamic drag and rotating mass under this condition. In 2018, Ning [33] also observed a dramatic increase in power with an increase in *LWC* values. The effect is more pronounced under glaze-ice conditions than under rime-ice conditions. The power requirements were almost doubled in the case of rime ice, whereas they increased by five times with glaze-ice conditions when the *LWC* value was varied from 0.5 $\frac{\mathrm{g}}{\mathrm{m}^3}$ to 2 $\frac{\mathrm{g}}{\mathrm{m}^3}$.

The lift ratio decreased with *LWC* under rime-ice conditions but was least affected by *LWC* at mixed ice temperatures, possibly due to the ogee wing tip effect. Experimental studies conducted by Benmeddour [32] in 2020 also depicted that a change in *LWC* has a more pronounced effect on icing characteristics than changes in MVD. As the value of *LWC* increased, the rate of decrease in thrust and the corresponding rate of increase in electrical power varied drastically with a constant MVD value of 20 µm. When the *LWC* was increased from $0.2\ \frac{g}{m^3}$ to $1\ \frac{g}{m^3}$, the time taken for a 50% reduction in thrust decreased by $(1/9)^{th}$ for a small blade (10″ dia), by $(1/6)^{th}$ for a medium blade (12″ dia), and by $(1/6)^{th}$ for a large blade (14″ dia). Correspondingly, the power requirements increased by approximately 65%, 55%, and 20% for the small, medium, and large blades, respectively. An increase in the rate of thrust degradation with *LWC* was also observed for SLD icing by Villeneuve in 2022 [42].

In 2018, Liu [43] extended his studies to understand the effects of ice-induced wake characteristics of the UAV propeller using a particle image velocimetry (PIV) technique. Additional measurements were performed to provide determine both the instantaneous flow characteristics and the ensemble-averaged flow statistics (e.g., mean velocity, vorticity, and turbulence kinetic energy) in the wake of the rotating propeller model. It was observed that the complex ice structures formed during glaze ice with increased *LWC* significantly disturb the wake flow field, resulting in the formation of larger and more complex vortices, which increases the drag and structural vibrations. Mean velocity, vorticity and turbulent kinetic energy varies marginally under rime-ice conditions, but significant variations were observed for glaze ice with increased *LWC*. The significant effect of *LWC* on the performance degradation of propellers was depicted in the work, but the effect of other parameters must also be considered for a better understanding.

3.3. Effect of MVD

For the rime-ice case at $T_\infty = -12$ °C, in 2020, Benmeddour [32] observed that a change in the MVD value from 20 µm to 60 µm with a constant *LWC* value of 0.5 g/m^3 had only a negligible influence on the rate of change of thrust, torque, and power. Similar observations were made by Kazomara [44] during an icing wind tunnel test of a multicopter UAV under mixed ice conditions ($T_\infty = -5$ °C). A power increase of 100% was obtained in 80 s for an MVD value of 20 µm, with the same result after 70 s for an MVD value 40 µm. Thus, an increase in MVD values can increase the rate of thrust reduction, but the effect is not prominent. The overall power requirements increase by 40% percent due to icing, but the power increment due to the increase in MVD is only around 5%. Most studies discussed in this review were based on FAR 25 Appendix C icing conditions. When Kazomara [44] performed studies based on Appendix O freezing drizzle conditions by increasing the MVD to 100 µm, the performance curves seemed unaffected when compared to the same conditions at 40 µm. In 2021, Catry [45] performed icing studies on a 9-inch-diameter three-blade propeller with an estimated MVD value of 400 µm at $T_\infty = -5$ °C. It was observed that the ice accreted with such high MVD values resulted in ragged ice features and complex 'lobster-tail-like' ice structures, as observed by Liu [16] and associated with a considerable increase in ice mass to 17 g within 65 s. At a rate of 25×10^{-3} N per sec ond, the thrust dropped from 1.65 N to zero in just 65 s. Thicker ice accretions and faster performance degradation were also observed by Villeneuve [42] in 2022 in association with high MVD values (supercooled large droplets). This may be due to the high inertia of the large droplets, which decreases the capability of such droplets to follow the streamlines, thereby increasing the collision efficiency.

3.4. Effect of RPM

In 2018, Yan [37] reported that increasing the RPM from 2000 to 3000 boosted the power requirements by 135% during the hovering state of a UAV in experiments performed under ice conditions of $T_\infty = -10$ °C. During experimental studies under rime-ice conditions conducted in 2021, Suurnäkki [46] also noted that increasing the RPM caused an increase

in the rate of water impingement, which, in turn, caused more ice to accumulate. Increased amounts of ice are observed to be accreted along the blade's tip, where the rotational speeds are higher. Higher rotational velocity increases the effective velocity of air relative to the propeller, which, in turn, increases the droplet impingement rate. In contrast, in 2021, Benmoddour [32] did not observe any significant changes in the time variations of the thrust, torque, or electrical power as ice accreted on the blades at 8000 rpm and 9000 rpm. Villeneuve [42] reported a decreased performance degradation with increased RPM under freezing drizzle ice conditions.

3.5. Effect of Free-Stream Velocity

In 2018, Yan [37] discovered that power loss increases with wind speed. Adding a 5 m/s wind velocity to a hovering UAV can result in a 67% increase in power at 3000 rpm. Suurnäkki [46] also observed an increased ice accretion rate with free-stream velocity in 2021. As a result, power and thrust changes under forward flight icing conditions may differ from those observed while hovering in an icing cloud. The increase in free stream velocity can also increase the advance ratio.

3.6. Effect of Advance Ratio

In 2021, Suurnäkki [46] performed experimental studies to understand the variation of the thrust coefficient and power coefficient as a function of advance ratio at two constant RPMs of 3000 and 5000. For both the RPMs, the thrust coefficient decreased with an increase in advance ratio. The experiments were conducted for an ice accretion duration of 5 min, and overall, the performance coefficients degraded with time. For 3000 the RPM case at low values of advance ratio (<0.5), the degradation of the thrust coefficient with time was negligible, but it increased with the advance ratio due to the increase in the rate of ice accretion. With higher values of advance ratios (>0.5) at this RPM, the thrust coefficient initially increases for some time before it degrades. This initial increase may be due to the increase in the effective chord due to rime-ice accretion, as observed in the case of fixed-wing UAVs [25]. At very high values of advance ratios of about 0.72, the thrust coefficient initially increased to 70% (compared to a clean propeller) before degrading to 10%. Similarly, the variations in the power coefficient were negligible for low values of the advance ratio and increased with an advance ratio up to 20%. For the 5000 RPM case, a steady decline in the thrust coefficient was observed over time, except at high values of the advance ratio, where a slight increase in thrust (10%) was observed before declining. Thrust loss of up to 50% was observed for very high values of the advance ratio of 0.69. The increase in power coefficient with time was also more evident at this higher RPM, and it became steeper at higher advance ratios. The power coefficient increased by 100% for the case with the highest advance ratio of 0.69. Highest RPM with highest advance ratio indicated the highest rate of icing, possibly due to the increased water impingement rates.

3.7. Effect of Propeller Diameter

Experimental studies conducted by Benmeddour [32] in 2020 on three propellers with diameters of 10″, 12″, and 14″ indicated that the blade with the smallest diameter was more tolerant to ice accretion than the larger blades. For all the scenarios considered in the study, the rate of decrease in thrust was also observed to increase with increased propeller diameter. The thrust degradation rate was almost doubled when the propeller diameter increased from 10″ to 14″ . A 50% reduction in thrust duration was selected as a criterion to stop the tests. During ice accretion, larger propellers dropped thrust at a faster rate than smaller propellers; therefore, the spraying time for the larger propellers were much shorter than for smaller propellers. As a result, the smaller propeller had more ice at the end of the test compared to the larger propellers. Icing studies with a fixed time duration are necessary to understand the diameter effect more accurately.

3.8. Effect of Blade Material

Experimental studies on carbon fiber (CF) blades with smooth surfaces and on plastic blades with a matte finish (the propeller blades are not identical) were performed by Yan [37] in 2018. Plastic blades have high ice adhesion strength compared to CF blades, so they collect ice at a higher rate. Furthermore, higher adhesion strength reduces the shedding of ice. Benmeddour [32] compared the ice accretion behavior of CF and glass fiber-reinforced plastic (GFR) propeller blades and observed that the thrust decreased more rapidly for the CF propeller blades than for the GFR blades. More runback ice was also observed on the GFR blades than on CF blades. Thus, carbon fiber blades have an increased rate of ice accretion relative to that of GFR blades due to their surface material characteristics such as roughness. In 2019, Li [47] reported that the dissipation of latent heat of fusion released during the solidification process was much slower for a thermoplastic substrate (due to its low thermal conductivity) compared to an aluminum substrate. Such a slow dissipation rate can lead to higher surface temperatures and a much longer freezing time. Thus, water runback on the surface is obvious, resulting in the formation of complex rivulet-like structures and more ice-covered areas. These studies were performed on a non-rotating substrate, and the influence of centrifugal force was not considered. Surface roughness and thermal conductivity are two important material properties that can affect ice accretion behavior. The effect of such material properties on RWUAV ice accretion remains a gap in the literature that needs to be understood in greater detail.

3.9. Effect of Angle of Sideslip and Tilt Angle

No considerable changes in the performance parameters were observed by Benmeddour [32] when he increased the angle of the sideslip by 30 degrees under rime icing conditions. Tilt angle is the angle between the rotational axis of the motor and the vertical line. Yan [37] commented that the tilt also influences the ice accretion rate, although the existing literature is insufficient to understand the effect, and this relationship remains a knowledge gap. Kazomara [44] performed ice tunnel experiments on a multicopter UAV at an angle of attack of 10 degrees. When comparing to the previous studies at zero-degree angle of attack, the pressure side of the propeller blade was consistently iced. This may be due to the increase in droplet impingement on the pressure side of the propeller blade when it is tilted nose-down. During the studies, it was also observed that ice formation occurred quite uniformly. There was no considerable difference between the ice accreted on the front and rear rotors. This is in contrast to the general preconception of expecting more ice on the windward side rotors. Yan [37] observed more ice accretion on the lower rotor than the upper rotor when he performed studies on coaxial rotors. Villeneuve [42] reported that a decrease in pitch is more detrimental to iced propeller aerodynamics.

Discussion: In contrast with the observations made during fixed-wing UAV icing [25], ice accretion on RWUAVs at temperatures very close to the freezing point ($T_\infty = -2\ ^\circ\mathrm{C}$) represent least threat to aerodynamic penalties. At warmer temperatures, the freezing time increases and is further augmented by aerodynamic heating of the propeller blade induced by the rotational speed. Thus, the droplets are more likely to drip from the surface before freezing. The effect of aerodynamic heating on RWUAVs is still not understood and is open to research. Mixed ice and rime-ice temperatures are more detrimental to aerodynamic performance of RWUAVs, the severity of which is determined by the complexity of the formed ice structures. Dramatic increases in power requirements were observed at mixed icing temperatures and can be considered detrimental to propeller icing. An increase in *LWC* values has a profound impact on thrust degradation and the power increment. The effect of MVD on RWUAV ice accretion can be considered negligible within in FAR 25 icing envelopes. RPM and V_∞ can influence RWUAV ice accretion in two ways: (1) The aerodynamic heating of the propeller blade is determined by the effective velocity, which, in turn, influences the fraction of unfrozen droplets. (2) The collision efficiency of the droplets also depends on RPM and V_∞. Studies show that increases in these parameters increase the rate of ice accretion and are therefore detrimental to aerodynamic performance under

rime-ice conditions. However, their effect is assumed to be more prominent at temperatures close to the freezing point, although this issue remains unstudied. Studies by Pecho [48] also indicate the significant effects of geometric parameters and material properties on propeller ice accretion. Consequently, such investigations and the effect of the direction of flow on RWUAV icing are an active and open area for research.

4. Ice Shedding

The ice layer is subjected to centrifugal forces due to the rotation of the propeller. Ice begins to shed when these forces overcome the adhesion force between the ice layer and the blade surface and cohesion force within the ice layer itself [42]. The shedding of ice causes an abrupt change in the blade's aerodynamic properties. Ice shedding events are frequently asymmetric in nature, resulting in mass imbalance and vibrations [37]. Upon shedding, the propeller suddenly regains its thrust, thereby decreasing the power requirements. Such abrupt changes can endanger UAV control and can also lead to structural failure. As a result, ice shedding events can be considered a risk for the operation of rotary-wing UAVs. Because of the heavy ice loads and high tip velocity, the ice section near the propeller blade tip experiences the greatest centrifugal force, resulting in early ice shedding. During propeller icing studies, multiple ice shedding events are observed, and this is reflected in the thrust curves as well.

The effect of various factors on ice adhesion strength was studied by Wang [49]. The adhesion strength of glaze ice increased with a reduction in temperature, but the trend was reversed at mixed and rime-ice temperatures. For glazing ice, the gradual freezing of water results in adequate surface wetting, and the ice–substrate link can be said to be in a Wenzel condition [50]. A lower temperature strengthened the chemical bonds between the molecules of ice and the substrate material. In addition, the residual stress at the interface decreased more quickly, resulting in enhanced interfacial adhesion. At rime or mixed ice temperatures, water immediately froze upon contact with the substrate surface. The lower the substrate's temperature, the faster it froze, making it more difficult for water to make complete contact with the substrate's surface. The connecting state between the ice and the substrate can be considered as Cassie [50]. The interface's mechanical interlocking effect was diminished. In addition, the actual contact area between the ice and substrate surface was also diminished since the ice was not immersed inside the surface microstructure. These two elements contributed to the deterioration of adhesion strength. Glaze ice seems to have a higher overall adhesion strength than rime ice and mixed ice. As the MVD climbed from 10 m to 70 m, the adhesion strength initially decreased before increasing. The increase in adhesion strength was almost linear as air speed increased, but the growth trend subsequently halted. High thermal conductivity and high surface roughness also enhance the adhesion strength of ice. Wang [49] also concluded that the adhesion strength was more influenced by substrate temperature and surface roughness, while wind speed and substrate type had less of an impact. Therefore, three primary factors influence the adhesion strength: the physical characteristics of the ice, the type of substrate material, and their connection condition. The icing temperature changed the characteristics of the ice, as well as the connection status, moving it from the Wenzel state to the Cassie state. Similarly, the nature of the substrate material and the status of the connection were both influenced by the surface roughness. The centrifugal force increases with mass and rotational speed but decreases with propeller blade diameter.

The effects of various icing parameters on RWUAV ice shedding can be deduced from research by Benmeddour [32]. Experimental ice accretion studies were performed on propeller blades with three different diameters at an rpm of 8000. It was observed that smaller propellers have a higher tendency to shed ice than larger propeller. Experimental studies carried out at $-12\ ^{\circ}C$ for various values of MVD and *LWC* revealed that ice shedding events are more likely to occur at lower MVD and *LWC* values. In contrast to the general understanding about high ice adhesion properties of glaze ice, in 2022, Muller [40] observed that ice shedding occurs earlier at lower temperatures, whereas it tends to occur later at

higher temperatures, as shown in Figure 5. In 2022, Karpen [35] also observed that glaze ice shed much earlier and more often compared to rime ice. The first glaze-ice shedding occurred after 120 s and about six times in 1100 s, whereas rime ice shed after 450 s and only twice. However, larger amounts (size) of ice are shed under rime-ice conditions because the shedding happens after a longer ice accretion time [40]. Han (2021) [36], as well as Pecho [48] and Hylmar [41] (2022) also reported more frequent ice shedding at glaze-ice temperatures compared to mixed or rime-ice cases. The decrease in the thrust due to ice accumulation was 50 to 65%;when the ice begins to shed, the thrust starts recovering up to 80% of its degraded value at $T_\infty = -2$ °C and up to 65% at $T_\infty = -5/-10$ °C. During an ice shedding event, the ice first sheds from the tip, then from the region closer to the center. Therefore, the radius of the propeller until wherethe ice remains shrinks with each subsequent ice shedding event. After the ice has shed from one section, it accumulates more ice until the ice mass has exceeded a certain threshold and begins to shed again [40]. The increase in RPM value also favors ice shedding. The surface finish of the propeller has a significant influence on the phenomenon of ice shedding. Carbon fiber blades are observed to shed ice much earlier than glass fiber blades due to the smooth surface finish [32]. Similar observations about carbon fiber blades were reported by Yan [37] in 2018.

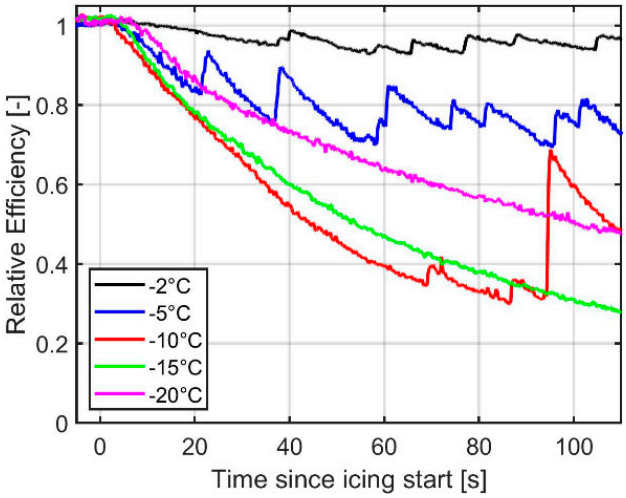

Figure 5. Effect of ice shedding on thrust curves [40].

Discussion: Ice shedding events have been shown to be more frequent at glaze-ice temperatures than at rime-ice temperatures, which goes against the popular belief that strong ice adhesion strength exists at these temperatures. Further research is required to fully comprehend this discrepancy between general knowledge and experimental observation. A significant increase in propeller vibration is observed during ice accretion, with increased vibration at warmer temperatures due to frequent shedding of ice compared to lower temperatures [41]. Initiating ice shedding by lowering the adhesion strength can be used as a passive method of ice mitigation. The effect of ice shedding on propeller vibration, the structural impact of shed ice on the propeller blade (hitting), and abrupt power changes due to ice shedding on the motor performance are not fully comprehended. Validation of existing numerical ice shedding models is also an important task to be addressed in this area.

5. Analytical Models for Ice Accretion on Propellers

Existing analytical and numerical models for the study of ice accretion on UAVs have significant limitations [25]. As a result, researchers have attempted to develop simplified models that can predict aerodynamic performance coefficients or ice thickness using datasets obtained from experimental studies. This section provides a brief overview of existing models.

In 2020, Yan [51] used experimental results to develop an empirical model to relate change in power (ΔP) to change in thrust (ΔT) as a function of the speed of propeller rotation (rpm), atmospheric temperature (T), and the time of ice accretion (t). Thrust and power changes are considered a linear function of the time of ice accretion, as expressed by:

$$\Delta P = \alpha(T,\ rpm).t \tag{2}$$

$$\Delta T = \beta(rpm).t \tag{3}$$

However, the empirical relations of α and β are specific to the operating conditions used in the experimental studies and therefore need to be validated for a wide range of conditions. To assess the effect of icing on flight performance and controllability, this model was integrated into a flight simulation model of a cargo UAV operating under icing conditions.

Liu in 2017, the authors of [16] presented an analytical model to calculate the ice thickness along the leading edge of a propeller blade as a function of time and blade span locations. For rime ice, the ice accumulation parameter (a) and growth rate $(da/d\tau)$ is expressed by [52]:

$$a = \frac{LWC.V_\infty.\tau}{d.\rho_i} \tag{4}$$

$$\frac{da}{d\tau} = \frac{LWC.V_\infty}{d.\rho_i} \tag{5}$$

where τ is the duration of ice accretion, d is the leading-edge diameter, and ρ_i is the ice density. For conditions with a constant V_∞, the rate of ice accumulation is directly proportional to LWC, as evidenced by the ragged ice formation at high values of LWC in the studies performed by Liu [16].

An analytical model to quantify the performance loss of a propeller with ice accretion was proposed by Müller [40] in 2022. This model can estimate ice accumulation, ice shedding forces, and the performance of an iced propeller. The model calculates thrust and torque as a function of the temperature, liquid water content, advance ratio, and the rotation rate of the propeller. To estimate the amount of ice accumulated on the propeller, a new term called total water collection (TWC) is introduced that combines the effect of LWC and icing duration (t):

$$TWC = t.LWC.\omega.\frac{d}{2} \tag{6}$$

where 'ω' is the rotation rate of the propeller, and 'd' is the propeller diameter. To account for the ice shedding, a factor called A_{max} is introduced, as expressed by:

$$A_{max} = TWC_{shedding}\frac{d}{2}\,\omega^2 \tag{7}$$

where $TWC_{shedding}$ is the maximum amount of ice on the propeller before shedding. The performance losses are calculated using:

$$C_T(T,\ TWC) = C_T(J) \times (1 + \min(TWC,\ TWC_{max}) \times \Delta C_T(T)) \tag{8}$$

$$\Delta C_T(T)) = \Delta C_{T,0} + \Delta C_{T,1}T + \Delta C_{T,2}T^2 \tag{9}$$

$$A_{max}(T) = A_{max,0} + A_{max,1}T^2 \tag{10}$$

$$TWC_{max}(n) = \frac{A_{max}}{2dn^2\,\pi^2} \tag{11}$$

where n is the rotational speed of the propeller, and $\Delta C_{T,0}$, $\Delta C_{T,1}$, and $\Delta C_{T,2}$ are the determined parameters required for thrust coefficient estimation. Similar equations are available for the power coefficient (c_P). The proposed model is based on second-order polynomial approximation from a series of experiments under different icing conditions

for a particular propeller configuration, as well as on assumptions for simplification of physics. Thus, the models need to be validated for a wide range of conditions, as well as geometric models.

In 2020, Scroger [53] proposed an empirical equation to predict the lift coefficient of an iced propeller; the correlation was derived from 36 experimental data points (under different environmental conditions) using multiple linear regression.

$$C_{l,ice} = \left[-1.311 \times \beta_0 \times A_c \times Re_\delta + 3809 \times \frac{T}{273.15} \times \theta_{Accr} + 28,413 \times \theta_{seg} - 4352\right] \times 10^{-4} \quad (12)$$

where β_0 is the stagnation line collection efficiency, A_c is an ice accumulation parameter, Re_δ id the Reynolds number based on droplet size, θ_{Accr} is the collective pitch angle of the ice accretion, and θ_{seg} is the collective pitch angle of a small ice segment considered for baseline measurements measured in radians. This equation was applied to a boundary element momentum theory (BEMT)-based code to predict the thrust and torque for an iced propeller. The model overpredicted the thrust by 33% and underpredicted the torque by 37%.

Discussion: The discussed analytical model mainly focuses on determining the aerodynamic penalties due to ice accretion on a rotating propeller based on the environmental conditions. The models are derived from experiments performed on a particular propeller model and are not universal. Therefore, all these models can be considered basic models that need to be improved to account for a wide range of geometric and environmental conditions.

6. Ice Mitigation Methods

The harmful impact of propeller icing on the aerodynamic performance of UAVs is evident from the previous sections. The sudden decrease in thrust and the associated increase in power due to ice accretion make UAV operations challenging during icing weather. Therefore, optimal ice mitigation systems must be developed to ensure all-weather-safe operation of UAVs. Aircraft icing protection systems (IPS) can operate in anti-icing mode and deicing mode. In anti-icing mode, the surface of the airfoil is heated continuously to avoid ice formation. In deicing mode, ice is allowed to accrete on the surface to a certain extent, and then heat is supplied periodically to remove the accreted ice. Electrothermal, electromechanical, and chemical IPS are typically utilized for the ice mitigation of UAVs. Muhammed [25] briefly discussed the pros and cons of each type of IPS for UAVs in 2021. Due to their small scale, high curvature, and high rotational speed, the development of IPS for small multirotor drone propellers presents additional challenges compared to their fixed-wing counterparts. A brief review of the IPS particularly suited for rotary-wing UAVs is provided in this section.

In 2017, Liu [54] conducted experimental investigations to understand the influence of surface wettability effects on dynamic ice accretion on UAV propellers. The experiments were conducted for glaze icing of hydrophilic and superhydrophobic surfaces. The surfaces were made superhydrophobic by applying commercially available superhydrophobic coatings. The contact angle was observed to be smaller than 90° ($\theta \approx 65°$) for a hydrophilic surface, and for a superhydrophobic surface, it was 157°. A water droplet impinging on a surface will flow only if an external force (shear force due to flow velocity or centrifugal force due to rotation) acting on the droplet can overcome the capillary force acting on the water droplet. It was found that the capillary force acting on the water droplets in a superhydrophobic surface is around 25 times lower than the same force acting on water droplets with a similar spherical cap radius on a hydrophilic surface. Thus, for the same air inflow conditions, the external force required to overcome the capillary forces is very small for superhydrophobic surfaces. Furthermore, the water droplets have less of tendency to stick and flow quickly over superhydrophobic surfaces without freezing compared to hydrophilic surfaces. The ice adhesion strength is approximately four times lower for superhydrophobic surfaces compared to hydrophilic surfaces. Ice accretion on superhydrophobic surfaces is observed to be much less than on hydrophilic surfaces.

However, considerable icicle structures were still observed along the superhydrophobic propeller's leading edge. This can be attributed to low or no shear stress near the stagnation line and therefore an inability to overcome the capillary forces. Furthermore, accumulation of ice occurs on the initial ice surface, as it is no longer hydrophobic. It is also interesting to note that a superhydrophobic coating can prevent any ice accretion on the surface of the propeller due to water runback, as the runback water flows off quickly. The performance penalties were observed to be less for superhydrophobic surfaces, with a 70% thrust coefficient gain and 75% lower power consumption than the corresponding hydrophilic surface for 100 s of icing. Villeneuve [55] tested four different hydrophobic coatings on an RWUAV propeller and observed that these coatings promote early ice shedding for both rime and glaze-ice conditions, although benefitting aerodynamic degradation under the glaze-ice condition only.

In 2022, Han [56] conducted experimental studies to compare the effectiveness of three different anti-icing coatings: a superhydrophobic coating (SHS), slippery liquid-infused porous surface (SLIPS) coating and stress-localized anti-icing (SLS) coating. SLS and SLIPS attempt to diminish the adhesion force of the ice; hence, the ice sheds more quickly. SHS prevents the droplet from adhering to the surface, causing it to fall away. It was observed that ice shedding happens frequently on SLS- and SLIPS-coated propellers for rime and glaze ice but less frequently on SHS-coated propellers. SLS- and SLIPS-coated propellers had shorter ice shedding intervals, and ice accumulation within the shedding interval was not very large. Consequently, when ice shedding occurs, the fluctuation in thrust is minor, resulting in consistent thrust. The power consumption was just 1.5 times more than that for a clean propeller. During the icing process, the SHS propeller power rose by a factor of 12 due to severe ice accretion, surpassing that of the clean propeller. Since the amount of ice accumulation during ice shedding for SHS is very high, the performance parameter fluctuations during ice shedding are also very high. The experimental results demonstrate that both low-adhesion coatings are successful at preventing icing, while the superhydrophobic surface's anti-icing performance is quite subpar. In 2021, Catry [45] tested a propeller with a transparent hybrid sol–gel coating (a silicon-based anti-icing coating) and observed that the coated propellers were able to maintain thrust for a longer time than the non-coated propellers. The coated propellers survived four times longer than the non-coated propellers.

In 2021, Muller [39] calculated the ice protection system loads on propeller blades under rime-ice conditions using numerical simulations for two different scenarios: running wet mode and fully evaporative mode. The former sets the surface temperature of the propeller at 0 °C, so the impinging droplets do not freeze, flowing downstream and shedding. In the latter case, the droplets need to be evaporated at the point of impingements, requiring more heat flux. Since the droplets evaporate upon impingement, only the impingent zones need to be heated. However, the water runback demands the heating of the entire propeller in the case of running wet condition. The required power in fully evaporative mode is observed to be 48% higher, while the maximum heat flux is 274% higher compared to the running wet mode. The heat flux values are observed to be higher near the leading edge, and the maximum is observed near the tip. Meteomatics GmbH developed a functional electrothermal anti-icing solution for their small-scale multirotor drones [26] in 2017.

In 2021, Hunt [57] proposed two methods for the deicing of multirotor UAV propellers: chemical coating and propeller reversal. Experimental studies were performed on a single two-blade propeller rotating inside environmental chambers to test the performance of the anti-icing methods. Eight different coatings were tested, and a reduction in ice accretion was observed, although it was not effective. Most coatings performed well in the initial phase but eventually failed to avoid the thrust drop because they were susceptible to wear during the icing cycle. Some ice was shed during the propeller reversal. Although the proposed methods have the ability to deice, their use in an effective manner requires further research.

In 2022, Karpen [35] developed a propeller-integrated electrothermal ice protection system (IPS) particularly suited for rotary-wing UAVs and tested it on a two-blade propeller model. It consists of a heating layer made of electrically conductive carbon ink screen-printed on interdigitated copper microelectrodes sandwiched between protective polymer coatings, as shown in Figure 6. The heat flux can be adjusted by varying the spacing of the electrodes. The space is reduced in regions demanding high heat flux, such as the tip of the propeller blade. Heat is generated in the carbon-filled ink when current is passed through it. The overall thickness of the panel is 150 µm, with a weight of 80 g, and is pasted on the surface of the propeller using adhesives. The IPS has a low heating power of 1 w cm^{-2} and is able to increase the temperature by only 5 °C. The IPS was tested under rime and glaze-ice conditions and was observed to be efficient only under the glaze-ice condition, whereas deicing under rime-ice conditions needed almost double the power.

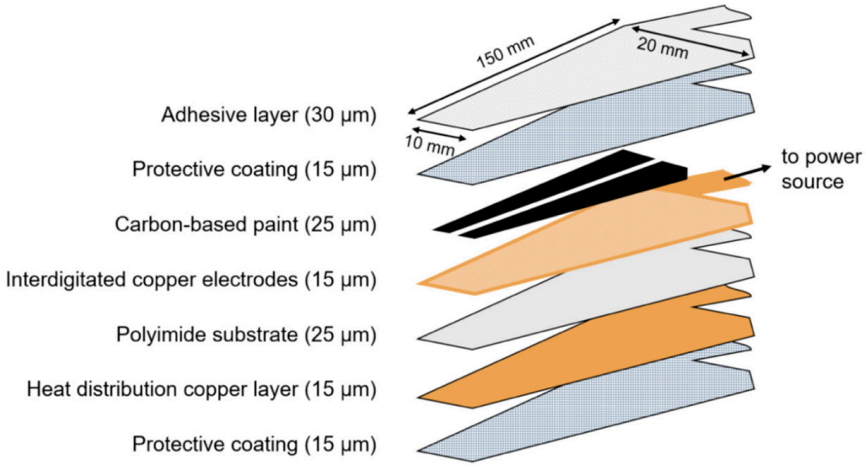

Figure 6. Propeller-integrated electrothermal IPS [35].

Piezoelectric materials exhibit strain-induced electric charge generation and electrical charge-induced strain generation. The former is referred to as a direct piezoelectric effect, while the latter is referred to as a converse piezoelectric effect. Because of this property, piezoelectric materials can be coupled with mechanical and electrical systems. There are two kinds of piezoelectric actuators: the first stimulates the actuator at an ultrasonic frequency (1 MHZ) [58], while the second induces structural resonance at a much lower frequency (below 1000 HZ) [59]. Palacios et al. [60] discovered that thermal effects due to vibrations were more likely to cause deicing than shear stress effects. In 2020, Villeneuve [61–63] studied the possibility of using piezoelectric actuators as a deicing system for small rotorcraft. During experimental testing, two forms of ice breaking were observed: cracking inside the ice layer (cohesive break) and delamination of the ice layer from the substrate (adhesive break).

7. Summary

The nature of ice accretion on RWUAVs differs from that on fixed-wing UAVs due to the following factors: (1) The surface water transport behavior is influenced by the centrifugal force, and water transport occurs along the spanwise direction. (2) The effective velocity experienced by the propeller blade is influenced by the propeller rotation speed (rpm), along with the free-stream velocity. An increase in effective velocity can increase the aerodynamic heating and the droplet collision efficiency. (3) Propeller icing is encountered by ice shedding events. (4) The linear increase in velocity from root to tip affects the rate of the ice accretion along the length of the blade. (5) The behavior of turbulent flow and associated wake region is also complicated by the rotational motion. The ice accretion behavior of RWUAVs is primarily governed by the T_∞, *LWC*, effective velocity, and material properties due to their influence on the water transport behavior. The interplay of T_∞

and *LWC* determines the fraction of water that remains unfrozen, and the centrifugal force and aerodynamic shear force govern its transport along the surface of the propeller blade. An increase in *LWC* at mixed ice temperatures can lead to the formation of complex "lobster-tail-like" ice structures that can reduce the thrust by 70% and increase the power consumption by five times. The surface roughness characteristics are highly altered by ice accretion and can increase the drag coefficient and power requirements. Kazomara [44] observed that the surface roughness due to ice accretion increases from root to tip and is minimum in the region between the leading edge and the trailing edge. The increase in surface roughness is also observed to increase with MVD. The highest RPM with the highest advance ratio indicates the highest rate of icing due to the increased water impingement rates. When the centrifugal forces overcome the adhesion force between the ice layer and the blade surface, ice starts shedding. T_∞, surface roughness, and propeller rotational speed can be considered major factors that govern this process. A database of various ice accretion studies on RWUAVs is provided in Table 1.

Methodologies used to study ice accretion on rotating propellers need additional features. The major requirements of an icing wind tunnels are:

1. Capability to conduct experiments for a wide range of environmental conditions and angles of attack;
2. Facility to measure and calibrate the liquid water content, mean volume diameter, and droplet distribution;
3. When using tunnels for rotary-wing structures, special instrumentations are needed to measure the thrust and torque of the propeller, as well as a technique to monitor the power consumption. Monitoring of power consumption is necessary for the optimum design of ice protection systems;
4. Instrumentation to measure the vibration of the propeller and the ice shedding frequencies;
5. Transient image capturing instruments are needed to photograph the ice shape at every instant, and 3D scanning techniques are needed obtain the ice shapes.

For numerical studies the major requirements are:

1. The numerical model must be capable of modelling the complex flow physics associated with the rotatory motion of propellers;
2. The effect of centrifugal forces on water droplets needs to be modelled;
3. The model must be capable of addressing the ice shedding phenomenon;
4. The capability of existing surface roughness models needs to be validated for RWUAVs, and more reliable models need to be developed;
5. The model should be capable of designing various surface characteristics and thermal properties of the substrate.

Among the major operating limitations of UAVs are power and size constraints. Therefore, the ice mitigations techniques used for RWUAVs must not be power-hungry. At present, no mature ice mitigation techniques exist for RWUAVs that can operate in a wide temperature range. The various electrothermal system used to date are effective only at temperatures close to the freezing point and draw more power under rime icing conditions. The use of various hydrophobic coatings can avoid excessive power consumption, but such coatings are sensitive to erosion effects, and their effectiveness diminishes rapidly. Studies were conducted to explore the possibility of using ultrasonic and piezoelectric vibration for deicing of rotary-wing structures such as helicopters, but their applicability to UAVs is yet to be determined. More compact models of such sensors need to be developed for application on small propeller blades.

Table 1. Database of ice accretion studies on RWUAVs.

Reference	Year	$Re \times 10^5$	Geometry	T_∞ (°C)	*LWC* (g/m^3)	MVD (µm)	V_∞ (m/s)	RPM	Advance Ratio	Time (S)	Comments
Meteomatics [26]	2017	-	Two-blade rotor	−2 −5 −5 −10 −10 −20	0.6 0.5 1.25 1.4 0.8 0.7	20 20 30 25 32.5 30	-	2000–7000	-	400	Increase in *LWC* values leads to more complex ice structures.
Liu [16,43,64,65]	2017 2018	$O(10^5)$	Three-blade propeller (200 mm)	−15 −5 −5	1 1 2	10–100	16	3000	≈0.25	115.8	Increase in *LWC* leads to complex "lobster-tail-like ice structures" and severe performance degradation.
Ning [33]	2018	$O(10^5)$	UAS propeller (240 mm)	−4 −8 −15	0.5, 1.0, 1.5, 2.0	10–100	10	4200	≈0.1	85	Lift degradation increases with decrease in atmospheric temperature. Increase in *LWC* also decreases thrust and increases power consumption by five times.
Yan [37,51]	2018 2019	-	Two-blade coaxial rotor 24.5 inch	−10	1.27	40	0	2000	-	60	With 60 s of icing, thrust decreases by 27.58%, and power consumption increases by 184%.
Benmeddour [24,32,66]	2020 2021	144,000	Two-blade 10-inch, 12-inch, and 14-inch propellers	−2 −5 −12	0.5 0.5 0.2, 0.5, 1.0	20 20 20, 40, 60	15	8000	0.37	Time of 50% reduction in thrust	Change in T_∞ and *LWC* had prominent effects on icing. A five times increase in *LWC* can make the thrust reduction five to eight times faster. Rime ice resulted in faster performance degradation.
Suurnäkki [45,67]	2020 2021	35,000 75,000	APC thin 11 × 8 two-blade propeller	−5	0.1	12–30	2–20 m/s	3000 5000	0.26, 0.29, 0.69, 0.72	300	Highest RPM with highest advance ratio is more detrimental to icing.
Scroger [53]	2020	-	14-inch CF two-blade rotor	−5, −10, −15, −20	0.692-1.1	20,40	-	2000 2500 3000	-	30, 45, 60	An empirical model was developed to predict airfoil lift degradation under icing conditions.
Villeneuve [61–63]	2020	-	Flat Plate	−8	-	-	-	-	-	-	The feasibility of a piezoelectric deicing system was studied.
Müller [39]	2020	50,000	21 × 10 propeller blade	−2 −5 −15	0.60 0.53 0.32	20	25	5000	0.65	120	The largest reduction in the efficiency of the propeller was achieved at a temperature of −5°.
Müller [40]	2021	-	21 × 13 2-blade propeller	−2, −5, −10, −15, −20	0.44		10–25	1750–5200	0.5–1.2	upto 300 s	The amount of ice grows with the decreasing temperature.

Table 1. *Cont.*

Reference	Year	$Re \times 10^5$	Geometry	T_∞ (°C)	*LWC* (g/m^3)	MVD (μm)	V_∞ (m/s)	RPM	Advance Ratio	Time (S)	Comments
Kazomara [44]	2021	-	Multicopter UAV	−20	0.86 0.86 1.5	20 40 100	20	2000	-	300	A 100% increase in required power and a 40 N decrease in lift were measured within 80 s of icing.
Catry [45]	2021	-	9 × 5 three-blad propeller	−10	-	400	6	3500	-	82	SLD can cause complex ice shapes with "lobster-tail-like ice structures".
Villeneuve [42]	2022	-	Bell APT70 drone rotor	−5, −12 −15	0.2 -7.5	120, 800	-	3880, 4440, 4950	-	300–800	SLD ice accretion on a hovering rotor was studied.
Hylmar [41]	2022	-	3D Robotics Solo propeller	−5, −10, −15	1.43 (g/s)	-	-	4000–7500	-	35	The power requirements increased by 505 % under rime-ice conditions.
Pecho [48]	2022	-	9 × 4.7, 8 × 4.5, 8 × 4 two-blade propellers	−2, −5 to −10	-	-	-	-	-	60	Thrust decreased by 65% due to ice accretion.
Han [36]	2022	-	DJI 9443	−5 −15	2 0.5	-	10	4200	-	427.5 837.8	Aerodynamic performance degradation was increased under rime-ice conditions after the first ice shedding event.
Han [56]	2022	-	DJI 9443	−5 −15	2 0.5	-	10	4200	-	440 1100	Low-adhesion coatings have a better anti-icing effect than SHS.
Villeneuve [55]	2022	-	Bell APT70 drone rotor	−5, −12	2.3, 6.3	120	-	3880, 4950	-	600	The use of hydrophobic coatings helps in early ice shedding.
Karpen [35]	2022	-	DJI 1345S two-blade propeller 33 cm	0	0.78	20	2.2	4000	-	1100	A higher thrust reduction rate of 1N/100 s was observed for glaze ice compared to 1N/250 s for rime ice.

8. Conclusions

Centrifugal force complicates ice accretion on rotary-wing UAVs compared to fixed-wing UAVs. The effect is more pronounced at warmer temperatures because of the fraction of water that remains unfrozen. These water droplets are carried by the action of centrifugal force and form complex ice structures, which can increase the surface roughness and induce flow separation and mass imbalance, thereby increasing drag and vibrations. A temperature range between −4 °C and − 10 °C with a high value of *LWC* seems to be the most dangerous icing condition for RWUAVs. High-speed transient imaging techniques are needed to better understand the ice shape evolution under various environmental conditions. Glaze ice is observed to have the least impact on RWUAV aerodynamic performance, whereas rime ice or mixed ice with high *LWC* values has the most impact. This is in contrast to the behavior of fixed-wing UAVs. The influence of atmospheric temperature and *LWC* on ice shape is understood in the existing literature, but the influence of various other parameters is yet to be understood. Ninety seconds of ice accretion can lead to a decrease in thrust by 70% and can increase the power consumption by 250% under glaze-ice conditions. For rime ice, the thrust coefficient can initially increase up to 70% before decreasing to 50%. Faster ice shedding occurs for glaze ice, and its rate is also amplified by the increase in rpm and decrease in propeller diameter. The smaller size, thin aerofoil structure, battery constraints, and rotating nature of the propellers demand unique ice mitigation techniques. Most existing electrothermal systems fail due to power constraints. The efficiency of a superhydrophobic coatings also seems to degrade drastically with ice shedding cycles. Low-adhesion surface coatings seem to be more promising technology for ice mitigation of RWUAVs than superhydrophobic coatings.

Author Contributions: Conceptualization, M.M. and M.S.V.; methodology, M.M.; investigation, M.M.; data curation, M.M.; writing—original draft preparation, M.M.; writing—review and editing, M.M.; supervision, M.S.V. All authors have read and agreed to the published version of the manuscript.

Funding: The work reported in this paper is supported by the UiT-The Arctic University of Norway (Project no-7400-72104) & nICE project of UiT & Research Council of Norway (Project no-324156).

Institutional Review Board Statement: Not applicable.

Informed Consent Statement: Not applicable.

Data Availability Statement: The data presented in this study are available upon request from the corresponding author.

Conflicts of Interest: The authors declare no conflict of interest.

References

1. Grogan, S.; Pellerin, R.; Gamache, M. The use of unmanned aerial vehicles and drones in search and rescue operations—A survey. In Proceedings of the PROLOG 2018, Hull, UK, 26 October 2018.
2. Aurambout, J.-P.; Gkoumas, K.; Ciuffo, B. Last mile delivery by drones: An estimation of viable market potential and access to citizens across European cities. *Eur. Transp. Res. Rev.* **2019**, *11*, 30. [CrossRef]
3. Goyal, R.; Reiche, C.; Fernando, C.; Serrao, J.; Kimmel, S.; Cohen, A.; Shaheen, S. *Urban Air Mobility Market Study*; UC Berkeley Library Office of Scholarly Communication Services: Berkeley, CA, USA, 2018. [CrossRef]
4. Villeneuve, E.; Karmouch, E.; Boulerice, X. Development of a small and transportable de-icing/anti-icing drone-mounted system. Part 1: System design. *Drone Syst. Appl.* **2022**, *10*, 155–177. [CrossRef]
5. Ucgun, H.; Yuzgec, U.; Bayilmis, C. A review on applications of rotary-wing unmanned aerial vehicle charging stations. *Int. J. Adv. Robot. Syst.* **2021**, *18*, 17298814211015863. [CrossRef]
6. Heaphy, M.; Watt, M.; Dash, J.; Pearse, G. UAVs for data collection-plugging the gap. *N. Z. J. For.* **2017**, *62*, 23–30.
7. Federal Aviation Administration. *FAA Aerospace Forecasts Fiscal Years 2021–2041*; Federal Aviation Administration: Washington, DC, USA, 2021.
8. Wild, G.; Murray, J.; Baxter, G. Exploring Civil Drone Accidents and Incidents to Help Prevent Potential Air Disasters. *Aerospace* **2016**, *3*, 22. [CrossRef]

9. Williams, K.W. *A Summary of Unmanned Aircraft Accident/Incident Data: Human Factors Implications*; Federal Aviation Administration Oklahoma City Ok Civil Aeromedical Inst.; Defense Technical Information Center; National Technical Information Service: Springfield, VA, USA, 2004.
10. Australian Transport Safety Bureau (ATSB). *An Analysis of Fixed-Wing and Rotary-Wing Aircraft Accidents Involving Private Operations 2001 to 2005*; Aviation Research and Analysis Report B2007/0099, Final; ATSB Transport Safety Investigation Report: Canberra, Australia, 2007.
11. Botura, G.; Fahrner, A. Icing Detection System-Conception, Development, Testing and Applicability to UAVs. In Proceedings of the 2nd AIAA "Unmanned Unlimited" Conference and Workshop & Exhibit, San Diego, CA, USA, 15–18 September 2003. [CrossRef]
12. Lundby, T.; Christiansen, M.P.; Jensen, K. Towards a Weather Analysis Software Framework to Improve UAS Operational Safety. In Proceedings of the 2019 International Conference on Unmanned Aircraft Systems (ICUAS), Atlanta, GA, USA, 11–14 June 2019; pp. 1372–1380.
13. Sørensen, K.L.; Borup, K.; Hann, R.; Bernstein, B.; Hansbø, M. UAV Atmospheric Icing Limitations; Research Report. 2021. Available online: https://www.ubiqaerospace.com/_files/ugd/5cc5ed_0d5872d85a2b4f1caa749eb05e4aeb4c.pdf (accessed on 1 November 2021).
14. Dilba, D. *Integrating Unmanned Drones and Air Taxis into the Airspace*; MTU Aero Engines Ag: Munich, Germany, 2021.
15. Tramposch, A.; Thomann, M.; Kozomara, D. Determination of Droplet Impingement on an Octocopter at Different Flight and Icing Conditions with Cfd Methods. In Proceedings of the Aiaa Aviation 2021 Forum, Virtual Event, 2–6 August 2021; American Institute of Aeronautics and Astronautics: Fairfax, VA, USA, 2021.
16. Liu, Y.; Li, L.; Ning, Z.; Hu, H. An Experimental Study on the Transient Ice Accretion Process over the Blade Surfaces of a Rotating UAS Propeller. In Proceedings of the 255th AIAA Aerospace Sciences Meeting, Grapevine, TX, USA, 9–13 January 2017.
17. Cao, Y.; Chen, K. Helicopter icing. *Aeronaut. J.* **2010**, *114*, 83–90. [CrossRef]
18. Lamraoui, F.; Fortin, G.; Benoit, R.; Perron, J.; Masson, C. Atmospheric icing impact on wind turbine production. *Cold Reg. Sci. Technol.* **2014**, *100*, 36–49. [CrossRef]
19. Peterson, A.; Dadone, L.; Bevan, A. *Rotorcraft Aviation Icing Research Requirements: Research Review and Recommendations*; NTRS-NASA Technical Reports Server: Philadelphia, PA, USA, 1981. Available online: https://ntrs.nasa.gov/citations/19810014537 (accessed on 1 November 2021).
20. NASA Glenn Research Centre. Rotorcraft Lcing. Available online: https://www1.grc.nasa.gov/aeronautics/icing/rotorcraft-icing/ (accessed on 5 February 2023).
21. Brouwers, E.W.; Palacios, J.L.; Smith, E.C.; Peterson, A.A. The experimental investigation of a rotor hover icing model with shedding. In Proceedings of the American Helicopter Society 66th Annual Forum, Phoenix, AZ, USA, 11–13 May 2010; pp. 1863–1875.
22. Hansman, R.J.; Kirby, M.S. Comparison of wet and dry growth in artificial and flight icing conditions. *J. Thermophys. Heat Transf.* **1987**, *1*, 215–221. [CrossRef]
23. Campbell, S.E.; Broeren, A.P.; Bragg, M.B. Sensitivity of Aircraft Performance to Icing Parameter Variations. *J. Aircr.* **2007**, *44*, 1758–1760. [CrossRef]
24. Benmeddour, A. *Investigation of Tolerance for Icing of small UAV Rotors/Propellers: Phase 1*; Aerospace: 2019/03/29; National Research Council of Canada: Ottawa, ON, Canada, 2019.
25. Muhammed, M.; Virk, M.S. Ice Accretion on Fixed-Wing Unmanned Aerial Vehicle—A Review Study. *Drones* **2022**, *6*, 86. [CrossRef]
26. Fengler, M. *Study of Propeller Icing Hazard in Mini-UAV Aviation*; Meteomatics GmbH Technical Report: St. Gallen, Switzerland, 2017.
27. Avery, A.S.; Jacob, J.D. Evaluation of Low Altitude Icing Conditions for Small Unmanned Aircraft. In Proceedings of the 9th AIAA Atmospheric and Space Environments Conference, Denver, CO, USA, 5–9 June 2017; p. 3929.
28. Siddique, M.A. An experimental study on the effects of adverse weathers on the flight performance of an Unmanned-Aerial-System (UAS). In *Graduate Theses and Dissertations. 18615*; Iowa State University: Ames, IA, USA, 2021. [CrossRef]
29. Dhulipalla, A.; Han, N.; Hu, H.; Hu, H. A Comparative Study to Characterize the Effects of Adverse Weathers on the Flight Performance of an Unmanned-Aerial-System. In Proceedings of the AIAA Aviation 2022 Forum, Chicago, IL, USA, 27 June–1 July 2022; American Institute of Aeronautics and Astronautics: Fairfax, VA, USA, 2022. [CrossRef]
30. Puffing, R.F.; Hassler, W.; Tramposch, A.; Peciar, M. *Ice Shape Mapping by Means of 4D-Scans*; 0148-7191; SAE Technical Paper: Minneapolis, MN, USA, 2015; p. 8.
31. Neubauer, T.; Kozomara, D.; Puffing, R.; Hassler, W. *Validation of Ice Roughness Analysis Based on 3d-Scanning and Self-Organizing maps*; 0148-7191; SAE Technical Paper: Minneapolis, MN, USA, 2019.
32. Benmeddour, A. *Investigation of Tolerance for Icing of Small UAV Rotors/propellers: Phase 2*; Aerospace: 2020/03/31; National Research Council of Canada: Ottawa, ON, Canada, 2020.
33. Ning, Z. *Experimental Investigations on the Aerodynamic and Aeroacoustic Characteristics of Small UAS Propellers*; Iowa State University: Ottawa, ON, Canada, 2018.
34. (EASA). Certification Specifications (CSs). Available online: https://www.easa.europa.eu/en/document-library/certification-specifications (accessed on 26 December 2022).
35. Karpen, N.; Diebald, S.; Dezitter, F.; Bonaccurso, E. Propeller-integrated airfoil heater system for small multirotor drones in icing environments: Anti-icing feasibility study. *Cold Reg. Sci. Technol.* **2022**, *201*, 103616. [CrossRef]

36. Han, N.; Hu, H.; Hu, H. An Experimental Investigation on the Dynamic Ice Accretion Process over the Blade Surface of a Rotating UAV Propeller. In Proceedings of the AIAA Scitech 2022 Forum, San Diego, CA, USA, 3–7 January 2022; American Institute of Aeronautics and Astronautics: Fairfax, VA, USA, 2021. [CrossRef]
37. Yan, S.; Opazo, T.; Palacios, J.; Langelaan, J.W.; Germain, L.D. Experimental evaluation of multi-rotor UAV operation under icing conditions. In Proceedings of the Annual Forum Proceedings-AHS International, Phoenix, AZ, USA, 14–17 May 2018.
38. Mantay, W.R.; Campbell, R.L.; Shidler, P.A. Full-scale testing of an Ogee tip rotor. In Proceedings of the Helicopter Acoustics, Hampton, VA, USA, 22–24 May 1978; Part 2; pp. 277–308.
39. Müller, N.; Hann, R.; Lutz, T. UAV Icing: Numerical Simulation of Propeller Ice Accretion. In Proceedings of the AIAA Aviation 2021 Forum, Virtual Event, 2–6 August 2021; American Institute of Aeronautics and Astronautics: Fairfax, VA, USA, 2021. [CrossRef]
40. Müller, N.C.; Hann, R. UAV Icing: A Performance Model for a UAV Propeller in Icing Conditions. In Proceedings of the AIAA Aviation 2022 Forum, Chicago, IL, USA, 27 June–1 July 2022; American Institute of Aeronautics and Astronautics: Fairfax, VA, USA, 2022. [CrossRef]
41. Hylmar, K.; Socha, V.; Kusmirek, S.; Hanakova, L.; Urban, D.; Spak, M. Effect of Icing on the Unmanned Aerial Vehicle Propulsion Systems. In Proceedings of the 2022 New Trends in Civil Aviation (NTCA), Prague, Czech Republic, 26–27 October 2022; pp. 115–122.
42. Villeneuve, E.; Samad, A.; Volat, C.; Béland, M.; Lapalme, M. Experimental Investigation of Icing Effects on a Hovering Drone Rotor Performance. *Drones* **2022**, *6*, 345. [CrossRef]
43. Liu, Y.; Li, L.; Chen, W.; Tian, W.; Hu, H. An experimental study on the aerodynamic performance degradation of a UAS propeller model induced by ice accretion process. *Exp. Therm. Fluid Sci.* **2019**, *102*, 101–112. [CrossRef]
44. Kozomara, D.; Neubauer, T.; Puffing, R.; Bednar, I.; Breitfuss, W. Experimental Investigation on the Effects of Icing on Multicopter UAS Operation. In Proceedings of the AIAA Aviation 2021 Forum, Virtual Event, 2–6 August 2021.
45. Catry, G.; Ceyhan, O.; Noca, F.; Bosson, N.; Bardazzi, L.J.; Marquez, S.; Jordaens, P.J.; Brandolisio, D. Performance Analysis of Rotorcraft Propulsion Units in a Combination of Wind and Icing Conditions. In Proceedings of the AIAA Aviation 2021 Forum, Virtual Event, 2–6 August 2021; American Institute of Aeronautics and Astronautics: Fairfax, VA, USA, 2021. [CrossRef]
46. Suurnäkki, P.; Tiihonen, M.; Jokela, T. UAV Icing: Low Reynolds Number Drone Propeller Performance During Dynamic Icing Process. In Proceedings of the AIAA Aviation 2021 Forum, Virtual Event, 2–6 August 2021; American Institute of Aeronautics and Astronautics: Fairfax, VA, USA, 2021. [CrossRef]
47. Li, L.; Liu, Y.; Zhang, Z.; Hu, H. Effects of thermal conductivity of airframe substrate on the dynamic ice accretion process pertinent to UAS inflight icing phenomena. *Int. J. Heat Mass Transf.* **2019**, *131*, 1184–1195. [CrossRef]
48. Pecho, P.; Jarošová, M.; Fodor, P.; Rostas, J. Experimental Analysis of the Effect of Icing an Unmanned Aerial Vehicles in Multicopter Configuration. In Proceedings of the 2022 New Trends in Civil Aviation (NTCA), Prague, Czech Republic, 26–27 October 2022; pp. 147–151.
49. Wang, Y.; Xiong, K.; Zhu, C.; Zhu, C.; Guo, R.; Chen, L. Research on Normal Ice Adhesion Strength in Icing Wind Tunnel. Available online: https://ssrn.com/abstract=4263761 (accessed on 1 November 2021).
50. Koishi, T.; Yasuoka, K.; Fujikawa, S.; Ebisuzaki, T.; Zeng, X.C. Coexistence and transition between Cassie and Wenzel state on pillared hydrophobic surface. *Proc. Natl. Acad. Sci. USA* **2009**, *106*, 8435–8440. [CrossRef]
51. Yan, S.; Opazo, T.; Langelaan, J.; Palacios, J. Experimental Evaluation and Flight Simulation of Coaxial-Rotor Vehicles in Icing Clouds. *J. Am. Helicopter Soc.* **2020**, *65*, 1–15. [CrossRef]
52. Anderson, D. Acceptable tolerances for matching icing similarity parameters in scaling applications. In Proceedings of the 39th Aerospace Sciences Meeting and Exhibit, Reno, NV, USA, 8–11 January 2001. [CrossRef]
53. Scroger, S.; Palacios, J.; Han, Y. Urban Air Mobility Rotor Icing Performance Characterization and Prediction. In Proceedings of the AIAA Aviation 2020 Forum, Virtual Event, 15–19 June 2020; American Institute of Aeronautics and Astronautics: Fairfax, VA, USA, 2020. [CrossRef]
54. Liu, Y.; Li, L.; Li, H.; Hu, H. An experimental study of surface wettability effects on dynamic ice accretion process over an UAS propeller model. *Aerosp. Sci. Technol.* **2018**, *73*, 164–172. [CrossRef]
55. Villeneuve, É.; Samad, A.; Volat, C.; Béland, M.; Lapalme, M. Experimental Assessment of the Ice Protection Effectiveness of Icephobic Coatings for a Hovering Drone Rotor. In Proceedings of the International Workshop on Atmospheric Icing of Structures, Montreal, QC, Canada, 19–23 June 2022. Available online: https://www.mcgill.ca/iwais2022/files/iwais2022/paperid085.pdf (accessed on 1 November 2021).
56. Han, N.; Hu, H.; Hu, H. An Experimental Investigation to Assess the Effectiveness of Various Anti-Icing Coatings for UAV Propeller Icing Mitigation. In Proceedings of the AIAA Aviation 2022 Forum, Chicago, IL, USA, 27 June–1 July 2022; p. 3964. [CrossRef]
57. Hunt, B.; Rawlins, C.; Hill, B. An Analysis of Blade Deicing Techniques for Multi-Rotor UAV Propellers. In Proceedings of the 2021 IEEE Aerospace Conference (50100), Big Sky, MT, USA, 6–13 March 2021; pp. 1–6. [CrossRef]
58. Ramanathan, S. An Investigation on the Deicing of Helicopter Blades Using Shear Horizontal Guided Waves. Ph.D. Thesis, The Pennsylvania State University, State College, PA, USA, 2005.
59. Venna, S.V.; Lin, Y.-J.; Botura, G. Piezoelectric Transducer Actuated Leading Edge De-Icing with Simultaneous Shear and Impulse Forces. *J. Aircr.* **2007**, *44*, 509–515. [CrossRef]

60. Palacios, J.; Smith, E.; Rose, J. Investigation of an ultrasonic ice protection system for helicopter rotor blades. In Proceedings of the American Helicopter Society 64th Annual Forum, Montreal, QC, Canada, 29 April–1 May 2008; pp. 609–618.
61. Villeneuve, E.; Volat, C.; Ghinet, S. Numerical and Experimental Investigation of the Design of a Piezoelectric De-Icing System for Small Rotorcraft Part 1/3: Development of a Flat Plate Numerical Model with Experimental Validation. *Aerospace* **2020**, *7*, 62. [CrossRef]
62. Villeneuve, E.; Volat, C.; Ghinet, S. Numerical and Experimental Investigation of the Design of a Piezoelectric De-Icing System for Small Rotorcraft Part 2/3: Investigation of Transient Vibration during Frequency Sweeps and Optimal Piezoelectric Actuator Excitation. *Aerospace* **2020**, *7*, 49. [CrossRef]
63. Villeneuve, E.; Volat, C.; Ghinet, S. Numerical and Experimental Investigation of the Design of a Piezoelectric De-Icing System for Small Rotorcraft Part 3/3: Numerical Model and Experimental Validation of Vibration-Based De-Icing of a Flat Plate Structure. *Aerospace* **2020**, *7*, 54. [CrossRef]
64. Liu, Y.; Li, L.; Ning, Z.; Tian, W.; Hu, H. Experimental Investigation on the Dynamic Icing Process over a Rotating Propeller Model. *J. Propuls. Power* **2018**, *34*, 933–946. [CrossRef]
65. Liu, Y.; Li, L.; Hu, H. Effects of Ice Accretion on the Aerodynamic Performance and Wake Characteristics of an UAS Propeller Model. In Proceedings of the AIAA 2018-3496. 2018 Atmospheric and Space Environments Conference, Atlanta, GA, USA, 25–29 June 2018. [CrossRef]
66. Benmeddour, A. Experimental Investigation of Tolerance for Icing of Small RPAS Propellers at High RPM. In Proceedings of the AIAA Aviation 2021–2675 Forum, Session: UAV & UAM Icing, Virtual Event, 2–6 August 2021. [CrossRef]
67. Suurnäkki, P.; Jokela, T.; Tiihonen, M. Applying an Icing Wind Tunnel for Drone Propeller Research, Validation of New Measurement Instrument. In *New Developments and Environmental Applications of Drones*; Springer: Berlin/Heidelberg, Germany, 2022; pp. 31–49.